

Cantilever stress measurements for pulsed laser deposition of perovskite oxides at 1000 K in an oxygen partial pressure of 10^{-4} millibars

J. Prempfer, D. Sander, and J. Kirschner

Max-Planck-Institut für Mikrostrukturphysik, Weinberg 2, D-06120 Halle/Saale, Germany

(Received 14 January 2015; accepted 19 February 2015; published online 5 March 2015)

An *in situ* stress measurement setup using an optical 2-beam curvature technique is described which is compatible with the stringent growth conditions of pulsed laser deposition (PLD) of perovskite oxides, which involves high substrate temperatures of 1000 K and oxygen partial pressures of up to 1×10^{-4} millibars. The stress measurements are complemented by medium energy electron diffraction (MEED), Auger electron spectroscopy, and additional growth rate monitoring by a quartz microbalance. A shielded filament is used to allow for simultaneous stress and MEED measurements at high substrate temperatures. A computer-controlled mirror scans an excimer laser beam over a stationary PLD target. This avoids mechanical noise originating from rotating PLD targets, and the setup does not suffer from limited lifetime issues of ultra high vacuum (UHV) rotary feedthroughs. © 2015 AIP Publishing LLC. [<http://dx.doi.org/10.1063/1.4913946>]

I. INTRODUCTION

The preparation of nanometer thin films has reached a high level of perfection. This is the basis for the reliable production of omnipresent devices in the areas of electronics¹⁻³ and data storage.⁴ Here, perovskite oxide films, based on their multiferroic functionality, play a pivotal role with promising applications, including sensors and actuators.⁵ However, the functional properties of films are affected by numerous factors. One potentially detrimental aspect is film stress. Film stress may induce structural defects^{6,7} and may ultimately lead to delamination of the film from its substrate.⁸ Thus, quantitative film stress measurements are highly beneficial to complement film characterization.⁹

An established procedure to measure film stress during growth exploits the stress induced curvature of a thin substrate. Capacitive¹⁰⁻¹² and optical measurements¹³⁻²⁰ of the resulting substrate deflection are used. We apply an optical two-beam curvature measurement,²¹ which was initially developed for applications at room temperature under ultra high vacuum conditions.²² The application of this technique to pulsed laser deposition (PLD) of perovskite oxides is challenging, as here high substrate temperatures of order 1000 K and significant oxygen partial pressures of 10^{-4} millibars are routinely applied.²³⁻²⁷ These operation conditions render thermal drift and oxidation processes of the sample holder as significant experimental challenges.

We successfully modified our stress measurement setup²¹ by introducing extended shielding of the filament and the sample heating stage to ensure reliable stress measurements under these conditions. In addition, we combined PLD and stress measurements with an *in situ* medium energy electron diffraction (MEED) experiment. The shielding at the sample stage suppresses light emission from the bright sample and its glowing filament to facilitate MEED measurements at high sample temperature. This allows to monitor the film deposition rate, which is mandatory for the reliable determination of film thickness, and consequently of film stress. The growth rate is

cross checked against results obtained by a quartz crystal film thickness monitor.

We present the first examples of stress and MEED measurements during PLD growth of BaTiO₃ and SrTiO₃ atomic layers at high sample temperatures of 1000 K and in oxygen partial pressures of up to 10^{-4} millibars. We measure film stress of order GPa, which is quantitatively ascribed to the epitaxial misfit between film and the Pd(001) substrate. The stress results indicate pseudomorphic growth in 5 unit cell thick films (2 nm), which marks the upper thickness range of this study.

In Sec. II, we provide an overview of the experimental setup and present details on the sample holder design. Section III presents results of stress and MEED measurements during SrTiO₃ growth by PLD on Pd(001).

II. EXPERIMENTAL SETUP

A. PLD setup, target, and substrate

PLD of BaTiO₃ and SrTiO₃ films is performed with a KrF excimer laser (Coherent COMPex Pro 50, wavelength 248 nm)²⁹ with 2 J/cm² laser fluence and 2 Hz repetition rate. We use a F, Kr, He, Ne premix gas³⁷ for filling the excimer laser. PLD is performed from stoichiometric BaTiO₃ and SrTiO₃ targets.^{32,33} We use 0.1 mm thin Pt(001) and Pd(001) single crystals as substrates,³⁸ which are 12 mm long and 2.5 mm wide. A detailed description of the substrate cleaning procedure by Ar-ion bombardment and annealing is given in a previous publication.³⁹ The PLD target and the substrate surface are aligned at an angle of 39°, as indicated in Fig. 1.

Often, rotating targets are used in PLD applications to ensure a homogeneous ablation process.⁴⁰ We follow a different approach, as shown in Fig. 1. We use a computer controlled mirror and a stationary target. This allows to scan the laser beam across the target. Thus, ultra high vacuum (UHV) rotary feedthroughs for the target are obsolete. Consequently, vibrations, originating from target movements,

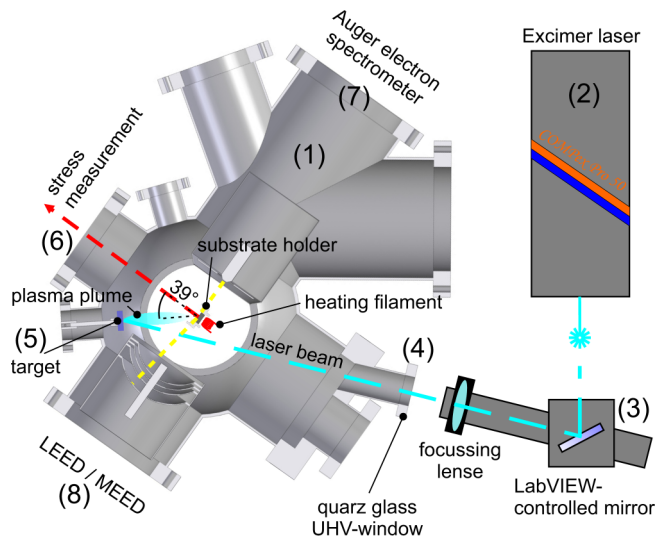


FIG. 1. Schematic overview of the UHV chamber²⁸ (1) and the excimer laser²⁹ (2) for PLD. We use PLD with a computer controlled mirror³⁰ (3) to scan the excimer laser pulses through an UV-transmitting window³¹ (4) across the target surface^{32,33} (5). The dashed blue line indicates the light path of the UV light used for PLD. The optical curvature measurement is mounted outside the UHV at the window flange (6).^{21,34} The red line indicates the light path of the optical curvature measurement. The substrate surface faces flange (6). The chemical composition of film and substrate are examined by an AES³⁵ mounted at flange (7), epitaxial order is investigated by LEED³⁶ at flange (8), where the screen is also used for MEED (8), with the electron beam of the AES.

are avoided and this helps to ensure low noise stress measurements. Also, we do not suffer from the limited lifetime of an UHV rotary feedthrough under continuous rotation. A further benefit of the stationary target is that we can use split targets, which contain different materials at different target locations. Thus, multilayers of different film materials can be produced by scanning the laser accordingly.

B. Sample holder for stress measurements

We modified the optical stress measurement setup over the last years, starting with a single beam,¹⁷ followed by a 2-beam curvature measurement^{43,44} where measurements at low temperatures (30 K) and in high magnetic fields²¹ are possible. With the sample holder described in Fig. 2, we now extend the temperature range to 1000 K.

An advantage of the 2-beam measurement over the single beam or capacitive deflection measurement is the direct determination of the stress induced curvature from the difference of two deflection signals. This ensures highly accurate results as this approach is much less affected by detrimental clamping effects.⁴⁵ Also, the inherent difference measurement of the two beam curvature measurement reduces noise and thermal drift effects markedly, leading to an improved signal-to-noise ratio.⁴⁶

The typical growth conditions for PLD of BaTiO₃ and SrTiO₃ films differ substantially from that of metal epitaxy, as high temperatures and high oxygen partial pressures are used.^{23–27} These conditions are experimentally demanding in view of thermal drift and oxidation of the sample holder.

Substrate temperatures of 1000 K in connection with the fairly large sample size applied here require heating powers

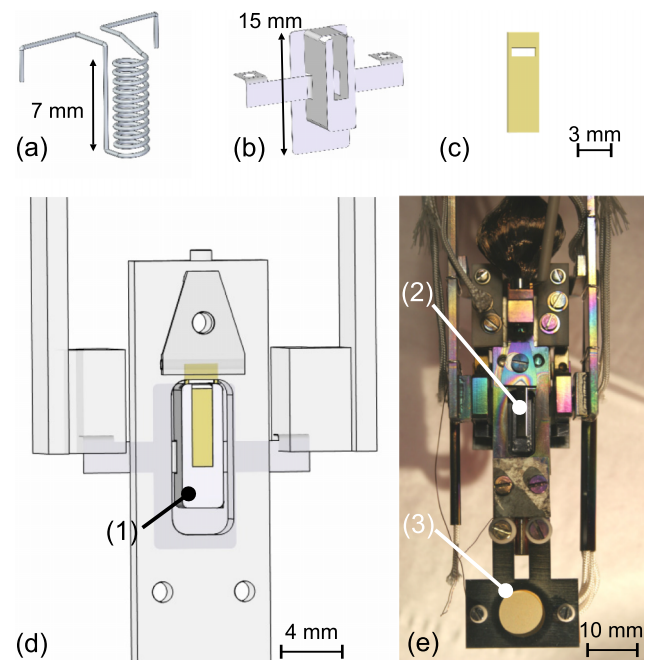


FIG. 2. (a) Schematic of the W-filament ($\varnothing=0.375$ mm), (b) filament shielding (0.25 mm Ta-foil, laser cut, and laser welded (shown also as (1) in (d)), and (c) W-foil placed between the filament and the sample rear side (0.1 mm, laser cut). (d) Schematic front view of the sample holder and (e) photograph with sample (2) and quartz oscillator (3) for thickness calibration.⁴¹ The sample holder provides a tilt for adjusting the sample normal, and it is part of a LHe cooled manipulator.⁴²

of order 100 W. To reach such high temperatures, high voltage (1000 V) assisted e-beam heating is usually applied, where the sample surface is at high positive potential and the filament is at ground potential. However, this heating method cannot be applied straightforwardly during MEED measurements. This is due to the deflecting action of the electrical potential applied to the substrate on the grazing electron beam of the MEED experiment. Therefore, the sample holder is modified such (see Fig. 2) that temperatures of 1000 K are reached by radiative heating only. With applied high voltage even higher temperatures of up to 2000 K can be reached.

High heating powers in addition to high oxygen partial pressures of $p_{O_2} = 1 \times 10^{-4}$ millibars lead unfortunately to a rapid oxidation of the W-filament, leading to a reduced lifetime. Furthermore, the substantial heat emitted by the filament does not only heat up the substrate, but it also leads to a slowly increasing sample holder temperature, causing thermal drift.

To address these experimental challenges, we designed a special W-filament (\varnothing 0.375 mm) shown in Fig. 2(a) with a corresponding shielding. The large W-wire diameter ensures an extended filament lifetime at 1000 K sample temperature of the order of several hours. Our filament shielding screens the filament thermally, electrically, and optically from the sample holder. We designed a shielding-“cage” (Fig. 2(b)) made of a 0.25 mm thin Ta-foil, which surrounds the filament. The opening of the “cage” in the direction to the substrate is closed by a 0.1 mm thick W-foil, see Fig. 2(c), without touching the “cage.” This part of the shielding is used for indirect radiative heating. The W-foil can be biased at a positive high voltage

for sample preparation, when no MEED experiments are performed. The low vapor pressure of W ensures a negligible evaporation of W onto the rear side of the substrate even at high temperatures. This is essential as we want to avoid stress variations with no deposition on the front substrate surface. The radiation shield is approximately at 1500 K for a sample temperature of 1000 K.

In the future, we are planning further improvements of our setup by implementing a transferable sample holder which includes the W-filament and the shielding parts. This will be beneficial in view of filament lifetime and maintenance.

Figure 2(d) shows schematically the present sample holder design without substrate crystal. The W-filament is located behind the shielding and remains invisible in this

sketch. The back of the sample holder is also covered by additional shielding parts, which are not shown here for clarity. A picture of the sample holder is given in (e) where substrate crystal (2) is mounted in front of the filament shielding. A quartz microbalance (3) is mounted at the lower end of the sample holder, and it allows independent growth rate measurements. This is beneficial in case that no MEED oscillations are observed during film growth and also for cross-checking the growth rate as derived from the MEED data.

This setup gives reliable stress measurements under typical PLD growth condition, as discussed next.

III. RESULTS AND DISCUSSION

A. Stress in SrTiO₃ films on Pd(001)

Figure 3(a) presents stress and MEED data taken during PLD of a SrTiO₃ film on Pd(001). The vertical dashed lines indicate when the PLD growth process started and stopped. In total, 400 pulses were fired onto the target within roughly 200 s. The stress curve (black, left scale) indicates an initial positive stress change in regime I for the first 40 s, before an almost constant negative slope of the stress signal is observed in regime II up to the end of deposition near 200 s.

The stress measurements are complemented by simultaneous MEED measurements (blue curve, right scale). We ascribe the local maxima of the MEED curve, as indicated by the vertical arrows, to the completion of a SrTiO₃ layer. The initial deposition in regime I leads to a sharp reduction of the MEED intensity, which recovers, giving rise to a first small relative maximum near 100 s, and showing slight local maxima with ongoing deposition, as indicated by the blue arrows. Ascribing tentatively the first maximum to the deposition of 2 unit cells (1 unit cell (uc) = 3.905 Å), we conclude that the total film thickness is 5 unit cells. This conclusion is corroborated by the thickness measurement by the quartz oscillator, presented in Fig. 4, which identifies a

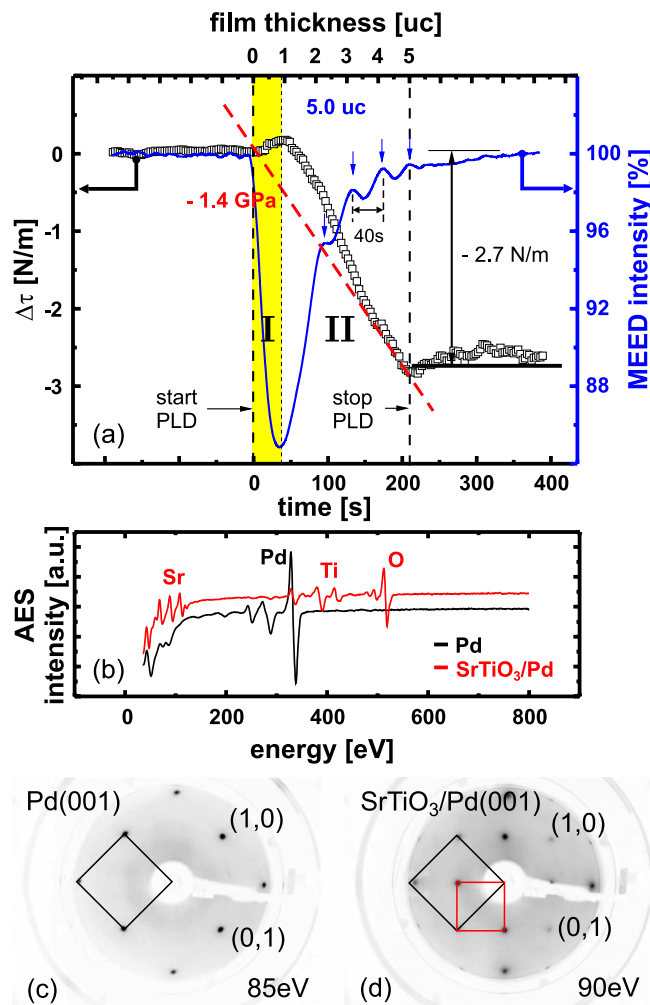


FIG. 3. (a) Stress change $\Delta\tau$ (open black squares) and MEED intensities (solid blue line) during PLD growth of 5 unit cells (uc) SrTiO₃ on Pd(001). Vertical lines indicate when the PLD deposition started and stopped (400 laser pulses, 2 Hz, $T_{\text{growth}} = 1000$ K, $p_{\text{O}_2} = 1 \times 10^{-4}$ millibars). The blue arrows indicate relative MEED maxima, indicative of filled layers. In regime I, a tensile stress change is observed, which changes to compressive in regime II after completion of the first unit cell. The slope of the dashed red line indicates a film stress of -1.4 GPa. Auger electron spectra obtained from the clean Pd substrate (Pd: 330 eV) and after SrTiO₃ film growth (Sr: 65 eV, 76 eV, 103 eV, 110 eV, Ti: 387 eV, 418 eV, O: 510 eV) are shown in (b). The LEED diffraction image (c) shows the characteristic 1×1 diffraction pattern of the clean substrate surface before PLD growth. (d) The diffraction pattern after growth shows a $c(2 \times 2)$ superstructure (smaller red square), where the 1×1 mesh is indicated (bigger black square).

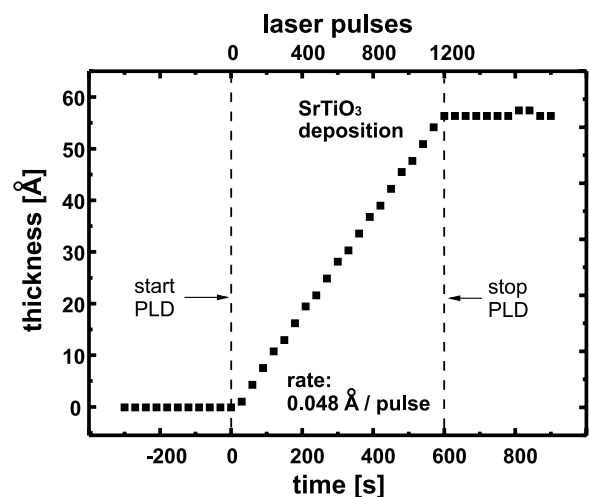


FIG. 4. Thickness measurement by the quartz oscillator.⁴¹ Vertical lines indicate when the PLD deposition started and stopped. A total of 1200 laser pulses on the SrTiO₃ target produce a thickness increase of 57 Å. This translates into a deposition rate of 0.048 Å per pulse (1 uc in 41 s at a repetition rate of 2 Hz). The SrTiO₃ film on Pd(001) in Fig. 3 is deposited with 400 pulses, which corresponds to 19.2 Å or 4.9 unit cells SrTiO₃.

TABLE I. Compilation of lattice misfit η and calculated film stress τ_{calc} based on room temperature bulk lattice constants and linear elasticity. The measured film stress τ_{exp} is given for comparison. The data for growth on Pt(001) are taken from another publication.^{39,47}

Stress in BaTiO ₃ and SrTiO ₃ films							
Substrate	Film	Film thickness (uc)	Lattice constant a_f (Å)	$\eta = \frac{a_s - a_f}{a_f}$ (%)	$\tau_{\text{calc}} = \frac{Y}{1-\nu} \cdot \eta$ (GPa)	τ_{exp} (GPa)	
Pt(001)	BaTiO ₃ _{cub}	18	4.012	-2.3	-4.3	-4.2	±0.4
$a_{\text{Pt}} = 3.920\text{Å}$	SrTiO ₃	7.5	3.905	+0.4	+1.4	+1.5	±0.2
Pd(001)	SrTiO ₃	5	3.905	-0.4	-1.4	-1.4	±0.2
$a_{\text{Pd}} = 3.890\text{Å}$							

deposition rate of one unit cell in 41 s. Thus, we obtain the thickness scale given at the top of the plot.

The film shows an epitaxial order, as indicated by the low energy electron deflection (LEED) image of Fig. 3(d), obtained after deposition of 5 unit cells. The growth is characterized by a compressive misfit, see Table I, and a compressive stress, i.e., a negative stress would be expected from the beginning of growth for epitaxial growth. The deposition of 5 uc SrTiO₃ leads to a stress change of -2.7 N/m . The average film stress is given by the slope of the red dashed line in Fig. 3 and it amounts to -1.4 GPa . This average stress is in quantitative agreement with the value calculated from epitaxial misfit as given in Table I.

Table I compiles the results of recent experimental film stress measurement τ_{exp} , lattice misfit η , and calculated film stress τ_{calc} ³⁹ and the result presented in Fig. 3. Tabulated film and substrate bulk lattice spacings (a_f, a_s) and elastic compliance constants s_{ij} of the film material were used to calculate η and τ_{calc} .³⁹

The epitaxial growth of SrTiO₃ on Pd(001) gives rise to a lattice misfit between SrTiO₃ and Pd(001) of -0.4% , which is due to the size mismatch between the respective surface unit cells of film and substrate. As a result, SrTiO₃ is expected to grow under compressive film stress with a calculated negative stress change of -2.65 N/m in a five unit cell thick film. This stress change is indeed observed quantitatively. This identifies lattice misfit as the dominant source of lattice stress in a 5 unit cell film, where the film maintains its integrity and epitaxial order at least to a thickness of five unit cells.

The observation of a non-monotonic stress change with tensile stress during deposition of the first unit cell of SrTiO₃ on Pd(001) comes as a surprise. In this thickness range, interface stress may dominate the stress response. A structural analysis by surface X-ray diffraction⁴⁸ for the similar system BaTiO₃/Pd(001) indicates an on-top bonding of O-atoms on Pd-atoms. We may assume the same interface structure and epitaxial order for SrTiO₃/Pd(001). This atomic arrangement of epitaxial growth gives rise to a $c(2 \times 2)$ -diffraction pattern,⁴⁸ in agreement with the LEED measurements of Fig. 3(c). It seems plausible, that the formation of O-metal bonds at the interface may lead to a stress, which deviates from misfit arguments. Possibly, this interface formation drives also the reduction of MEED intensity.

Auger electron spectroscopy (AES) shown in Fig. 3(b) confirms clean surface conditions of the Pd substrate before growth, and the typical AES spectra for SrTiO₃ are observed

after growth.³⁹ Thus, we rule out a surface contamination as the origin of the unexpected stress behavior in regime I.

The initial tensile stress and the sharp decay of the MEED intensity in regime I up to one unit cell suggest an interface formation which deviates from a simplistic expectation of strained layer-by-layer growth, which is the basis of the stress calculation. A change of growth mode leading to flat film layers seems to be favored after the deposition of one unit cell SrTiO₃. We conclude that misfit is the decisive contribution to film stress only in films thicker than one unit cell. The stress change induced by the first deposited unit cell is governed by interfacial stress of as of yet largely unexplored origin. Further studies are currently under way to elucidate the structural details of the SrTiO₃-Pd interface formation, where additional interfacial oxygen might play a dominant role.⁴⁸

IV. CONCLUSIONS

Optical cantilever curvature measurements are well suited to provide quantitative data on film stress during PLD of perovskite materials where high temperature and large oxygen partial pressures are required to ensure epitaxial growth. We find film stress of magnitude GPa in several unit cells thin films of the prototypical perovskite materials BaTiO₃ and SrTiO₃ on Pd(001) and Pt(001). The magnitude of stress in several unit cell thick films is ascribed to epitaxial misfit between film and substrate. In one unit cell thin films, other, up to now, unidentified stress contributions need to be considered to explain the observed stress. Stress measurements during film growth can be used to monitor the growth process *in situ* with sub-unit cell thickness sensitivity. This gives quantitative insights into stress-strain relations in atomic layer thin films.

ACKNOWLEDGMENTS

Partial support by SFB 762 is gratefully acknowledged.

- ¹L. Martin, Y.-H. Chu, and R. Ramesh, *Mater. Sci. Eng., R* **68**, 89 (2010).
- ²P. Zubko, S. Gariglio, M. Gabay, P. Ghosez, and J.-M. Triscone, *Annu. Rev. Condens. Matter Phys.* **2**, 141 (2011).
- ³M. Bibes, J. E. Villegas, and A. Barthelemy, *Adv. Phys.* **60**, 5 (2011).
- ⁴K. Abe, N. Yanase, K. Sano, M. Izuha, N. Fukushima, and T. Kawakubo, *Integr. Ferroelectr.* **21**, 197 (1998).
- ⁵A. J. Bell, *J. Eur. Ceram. Soc.* **28**, 1307 (2008).
- ⁶K. Wandelt, *Surf. Sci.* **251-252**, 387 (1991).
- ⁷P. Varga, E. Lundgren, J. Redinger, and M. Schmid, *Phys. Status Solidi (a)* **187**, 97 (2001).

- ⁸M. Hu, M. Thouless, and A. Evans, *Acta Metall.* **36**, 1301 (1988).
- ⁹F. Spaepen, *Acta Mater.* **48**, 31 (2000).
- ¹⁰R. Koch, H. Leonhard, and R. Abermann, *Thin Solid Films* **89**, 117 (1982).
- ¹¹R. Koch, H. Leonhard, G. Thurner, and R. Abermann, *Rev. Sci. Instrum.* **61**, 3859 (1990).
- ¹²D. Sander and H. Ibach, *Phys. Rev. B* **43**, 4263 (1991).
- ¹³A. J. Schell-Sorokin and R. M. Tromp, *Phys. Rev. Lett.* **64**, 1039 (1990).
- ¹⁴R. E. Martínez, W. M. Augustyniak, and J. A. Golovchenko, *Phys. Rev. Lett.* **64**, 1035 (1990).
- ¹⁵J. A. Ruud, A. Witvrouw, and F. Spaepen, *J. Appl. Phys.* **74**, 2517 (1993).
- ¹⁶P. Müller and R. Kern, *Surf. Sci.* **301**, 386 (1994).
- ¹⁷D. Sander, A. Enders, and J. Kirschner, *Rev. Sci. Instrum.* **66**, 4734 (1995).
- ¹⁸J. Floro, E. Chason, S. Lee, R. Twisten, R. Hwang, and L. Freund, *J. Electron. Mater.* **26**, 969 (1997).
- ¹⁹T. Scharf, J. Faupel, K. Sturm, and H.-U. Krebs, *J. Appl. Phys.* **94**, 4273 (2003).
- ²⁰P. Kury, T. Grabosch, and M. H. von Hoegen, *Rev. Sci. Instrum.* **76**, 023903 (2005).
- ²¹J. Premper, D. Sander, and J. Kirschner, *Rev. Sci. Instrum.* **83**, 073904 (2012).
- ²²D. Sander, *Rep. Prog. Phys.* **62**, 809 (1999).
- ²³A. Visinoiu, M. Alexe, H. N. Lee, D. N. Zakharov, A. Pignolet, D. Hesse, and U. Gösele, *J. Appl. Phys.* **91**, 10157 (2002).
- ²⁴J. Schwarzkopf and R. Fornari, *Prog. Cryst. Growth Charact. Mater.* **52**, 159 (2006).
- ²⁵B. R. Kim, T.-U. Kim, W.-J. Lee, J. H. Moon, B.-T. Lee, H. S. Kim, and J. H. Kim, *Thin Solid Films* **515**, 6438 (2007).
- ²⁶A. Khodan, S. Guyard, J.-P. Contour, D.-G. Crété, E. Jacquet, and K. Bouzehouane, *Thin Solid Films* **515**, 6422 (2007).
- ²⁷T. Ohnishi, T. Yamamoto, S. Meguro, H. Koinuma, and M. Lippmaa, *J. Phys.: Conf. Ser.* **59**, 514 (2007).
- ²⁸PINK GmbH Vakuumtechnik, Gyula-Horn-Str. 20, D-97877 Wertheim-Reinhardshof, Germany, <http://www.pink.de>.
- ²⁹Coherent Lambda Physik GmbH, Hans-Böckler-Strasse 12, D-37079 Göttingen, Germany, <http://www.coherent.com>.
- ³⁰Precision Tilt Stage M-041.D01 + Mercury Servo Controller C-863.11, PI, Physik Instrumente GmbH & Co. KG, Römerstraße 1, 76228 Karlsruhe, Germany, <http://www.pi.ws>.
- ³¹Quarzglas (Fused Silica) VPCF40-DUVQ-L, VACOM Vakuum Komponenten & Messtechnik GmbH, Gabelsbergerstraße 9, 07749 Jena, Germany.
- ³²BaTiO₃, 99.9%, ø 25 mm x 3 mm; MaTeck GmbH, Im Langenbroich 20, D-52428 Jülich, <http://www.mateck.de>.
- ³³SrTiO₃, 99.9%, ø 25 mm x 3 mm; MaTeck GmbH, Im Langenbroich 20, D-52428 Jülich, <http://www.mateck.de>.
- ³⁴D. Sander, Z. Tian, and J. Kirschner, *J. Phys.: Condens. Matter* **21**, 134015 (2009).
- ³⁵EK-5- IK + DESA 100, STAIB INSTRUMENTS GmbH, Hagenaustr. 22, D-85416 Langenbach, Germany, <http://www.staibinstruments.com>.
- ³⁶Omicron SpectraLEED, Omicron NanoTechnology GmbH, Limburger Strasse 75, D-65232 Taunusstein, Germany, <http://www.omicron.de>.
- ³⁷Premix 248 nm, 0.13% Fluor, 2.44% Helium, 3.42% Krypton, Rest Neon, 20 l, 110 bar, Ventilanschluß 8 VA; Linde AG Geschäftsbereich Linde Gas, Gradestr. 107, 12347 Berlin, Germany.
- ³⁸MaTeck GmbH, Im Langenbroich 20, D-52428 Jülich, <http://www.mateck.de>.
- ³⁹J. Premper, D. Sander, and J. Kirschner, “*In situ* stress measurements during pulsed laser deposition of BaTiO₃ and SrTiO₃ atomic layers on Pt(0 0 1),” *Appl. Surf. Sci.* (published online).
- ⁴⁰H. M. Christen and G. Eres, *J. Phys.: Condens. Matter* **20**, 264005 (2008).
- ⁴¹MANUAL - XTC/2 Deposition Controller, Leybold Inficon Inc., Two Technology Place East Syracuse, New York 13057-9714, <http://www.inficon.com> (1993).
- ⁴²CryoVac Gesellschaft für Tieftemperaturtechnik mbH & Co. KG, Heuserweg 14, 53842 Troisdorf, Germany, <http://www.CryoVac.de>.
- ⁴³D. Sander, S. Ouazi, A. Enders, T. Gutjahr-Löser, V. S. Stepanyuk, D. I. Bazhanov, and J. Kirschner, *J. Phys.: Condens. Matter* **14**, 4165 (2002).
- ⁴⁴D. Sander, Z. Tian, and J. Kirschner, *Sensors* **8**, 4466 (2008).
- ⁴⁵K. Dahmen, S. Lehwald, and H. Ibach, *Surf. Sci.* **446**, 161 (2000).
- ⁴⁶T. Gutjahr-Löser, “Magnetoelastische Kopplung in oligatomaren Filmen,” Ph.D. thesis (Martin-Luther-Universität Halle-Wittenberg, 1999).
- ⁴⁷J. Premper, “Mechanische Spannungen von BaTiO₃ und SrTiO₃ Atomlagen auf Metalleinkristallen,” Ph.D. thesis (Martin-Luther-Universität Halle-Wittenberg, 2014).
- ⁴⁸H. L. Meyerheim, A. Ernst, K. Mohseni, I. V. Maznichenko, J. Henk, S. Ostanin, N. Jedrecy, F. Klimenta, J. Zegenhagen, C. Schlueter, I. Mertig, and J. Kirschner, *Phys. Rev. Lett.* **111**, 105501 (2013).